Measurements of Laser Impulse Coupling at 130fs

Claude R. Phipps*[a], James R. Luke[b], David J. Funk[c], David S. Moore[c], James Glownia[c] and Thomas Lippert[d]
[a]Photonic Associates; [b]NMT/Institute for Engineering Research and Applications
[c]Los Alamos National Laboratory, [d]Paul Scherrer Institut

ABSTRACT

For the first time, we have measured the momentum coupling coefficient and plasma expansion velocity (specific impulse) in the femtosecond region, over a laser intensity range from ablation threshold to thirty times threshold. These measurements extend the laser pulsewidth three orders of magnitude relative to previous reports. We studied several pure metals and three organic compounds as targets. The organic compounds were exothermic polymers specifically developed for the micro-laser plasma thruster, and two of these used "tuned absorbers" rather than carbon particles for the laser absorption function. The metals ranged from Li to W in atomic weight. We measured time of flight profiles for ions and found dramatic two-temperature distributions for some conditions. Specific impulse reached record values for this type of measurement and ablation efficiency was near 100%.

1. MOTIVATION

Unknown as a field prior to 1972 [1], laser ablation propulsion is now progressing rapidly. Probably the first practical applications is the micro laser plasma thruster (μLPT)[6,8,11], but many other applications for transferring momentum to an object at distance have been considered[2-5,7,9,10]. For any of these, it is crucial to know how the laser fluence for maximum momentum transfer efficiency (dyn-s/J) depends on laser pulse duration.

Because momentum transfer efficiency decreases above the intensity for forming a fully ionized plasma due to plasma shielding, an optimum fluence exists. The grey diagonal bar in Figure 1 shows our best idea of this relationship prior to obtaining the data reported here. This is

$$\Phi = B\,\tau^{m} \quad J/cm^2 \qquad (1)$$

As is seen from the Figure, optimum fluence is reasonably independent of laser wavelength and material. This is because, when plasma is formed over a surface, a precondition for efficient momentum transfer, the properties of the plasma above matter more rather than those of the material beneath[12].

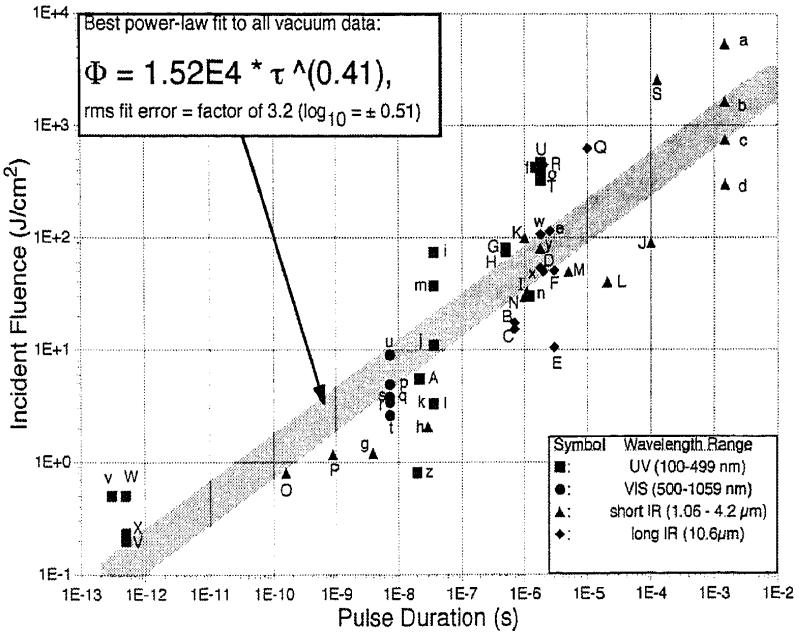

Figure 1. Literature values from 51 data sets established the trend indicated for Φ_{opt}. The points v,W,x,V were deduced from Q* data in the absence of coupling measurements at this pulse duration. Literature sources denoted by letters are catalogued in Ref. 7.

Simple 1-D thermal transfer theory[14] would predict an exponent m=0.5. The trendline deviates from that slope due to inclusion of points in the sub-ps region which were deduced from published etch depth maxima using a technique reported earlier[15]. The motivation for our measurements was that no measurements of impulse delivery to surfaces in vacuum previously existed for pulsewidths <100ps. Also, no model exists for predicting these parameters in the fs region.

*Corresponding author: crphipps@aol.com; phone/fax 1-505-466-3877; http://members.aol.com/crphipps/PA/PA.html; Photonic Associates, 200A Ojo de la Vaca Road, Santa Fe NM 87508

High-Power Laser Ablation V, edited by Claude R. Phipps, Proceedings of SPIE
Vol. 5448 (SPIE, Bellingham, WA, 2004) · 0277-786X/04/$15 · doi: 10.1117/12.568419

2. MODEL FOR τ >10ps

Laser-ablation-induced momentum transfer to a surface in vacuum is well described by a set of simple relationships based on theory for inertially confined fusion[12]. The theory predicts values for C_m, the momentum transfer efficiency (dyn-s/J) and I_{sp}, = v_E/g_o the "specific impulse" or exhaust velocity divided by the acceleration of gravity at Earth's surface, to within a factor of two under most conditions. This theory is valid down to $\tau \approx 10$ps, as was recently shown by Ihlemann[16].

Plasma absorbs laser radiation via inverse bremsstrahlung [i.e., absorption due to inelastic scattering of photons by free electrons and becomes more dense until the "critical electron density"

$$n_{ec} = m_e n^2 \omega^2 / 4\pi e^2 = 1.115\ E21/\lambda_{\mu m}{}^2 \qquad cm^{-3}. \tag{2}$$

is reached, where $\lambda_{\mu m}$ indicates the laser wavelength in μm. It can be shown that the effective thickness of the absorption zone is about $1/\alpha_{IB}$, where α_{IB} is the inverse bremsstrahlung absorption coefficient.

$$\alpha_{IB} \cong (\nu_{ei}/c)(n_e/n_{ec}) \tag{3}$$

Surface plasma formation provides very high absorption. In local thermodynamic equilibrium[9] , and in the limit $\nu_{ei}/\omega << 1$, and $n \approx 1$ (valid for vacuum propagation), we have the familiar formula for the laser absorption depth:

$$x_\alpha = \frac{1}{\alpha_{IB}} = \left(\frac{\nu_{ei}\, n_e}{c\, n_{ec}}\right)^{-1} = \frac{2^{5/2} c \sqrt{m_e}\, k^{3/2} n_{ec} T_e^{3/2}}{\pi^{3/2} Z e^4 n_e^2 \ln\Lambda} = b \frac{n_{ec} T_e^{3/2}}{n_e^2} \tag{4}$$

which decreases with the square of the wavelength, much smaller than the optical absorption depth in room temperature transparent materials, more like that in metals. The equivalent thickness of the absorption zone can be as small as a wavelength of the incident laser light. For example, at the KrF laser wavelength, 2eV plasma temperature and $n_e = 0.2\ n_{ec} = 3.3 \times 10^{21}$ /cm^3, we find $1/\alpha = \lambda = 248$ nm.

The second process that occurs due to the mediation of plasma absorption at the target surface is UV conversion: much or even most of the light actually reaching the surface is UV with a peak radiation wavelength

$$\lambda_{max} = 0.250/T_{e(eV)} \qquad \mu m. \tag{5}$$

Since plasma electron temperatures are often several eV, this is hard UV.

Our theoretical model[8] for determining surface pressure, electron temperature, coupling coefficient and mass ablation rate in the vacuum-plasma regime is now widely accepted.

In this model, the momentum coupling efficiency C_m (the ratio of ablation momentum produced to incident pulse energy) for essentially all "surface-absorbing" materials in vacuum irradiated at any of the usual wavelengths at or above plasma threshold intensity can be estimated to within a factor of 1.5 from the expression

$$C_m = 5.83 \bullet \frac{\Psi^{9/16} / A^{1/8}}{(I \lambda \sqrt{\tau})^{1/4}} \qquad dyn\text{-}s/J. \tag{6}$$

In Eqn (6), ($\Psi = (A/2)[Z^2(Z+1)]^{-1/3}$), Z is the average charge state of the laser-produced plasma, I, τ and λ are laser intensity, pulse duration and wavelength and A is target atomic mass. In addition, many transparent materials obey the same model when intensity is high enough to form a surface plasma at the beginning of the pulse. The only significant effort involved in interpreting this deceptively simple formula is that in determining average ionization state Z of the ablation ejecta, which is done using a Saha equation. Other results for electron temperature, density and velocity near the critical density surface are shown in Eqs. (7) - (9).

$$T_e = 2.98E4 \frac{A^{1/8} Z^{3/4} (I\lambda\sqrt{\tau})^{1/2}}{(Z+1)^{5/8}} \qquad K \tag{7}$$

$$n_e = 3.59E11 \frac{A^{5/16} I^{1/4}}{Z^{1/8} (Z+1)^{9/16} \tau^{3/8} \lambda^{3/4}} \qquad cm^{-3}. \tag{8}$$

and

$$I_{sp} = 1.4E3 \ \frac{A^{1/8}}{\Psi^{9/16}} (I \lambda \sqrt{\tau})^{1/4} \tag{9}$$

These relationships are valid above the threshold for plasma formation $\Phi > \Phi_{plas}$. Clearly, the C_m relationship (6) blows up if $\Phi \rightarrow 0$. Energy conservation requires that constant product relationships exist, in the monoenergetic stream limit:

$$2E7\eta_{AB} = \Delta m v_E^2/W = C_m^2 Q^* = g_o C_m I_{sp} = C_m v_E. \quad (10)$$

and that

$$C_m I_{sp} \leq 2E7/g_o = 2.04E4, \quad (11)$$

and physics prohibits results that violate these relationships strongly.

3. EXPERIMENTAL SETUP

Figure 2 shows the setup we used for these measurements. Laser pulse duration was 130fs ± 10fs at 800nm wavelength, and pulse energy was 20mJ. Calibrated reflective attenuators were used to vary pulse energy on the

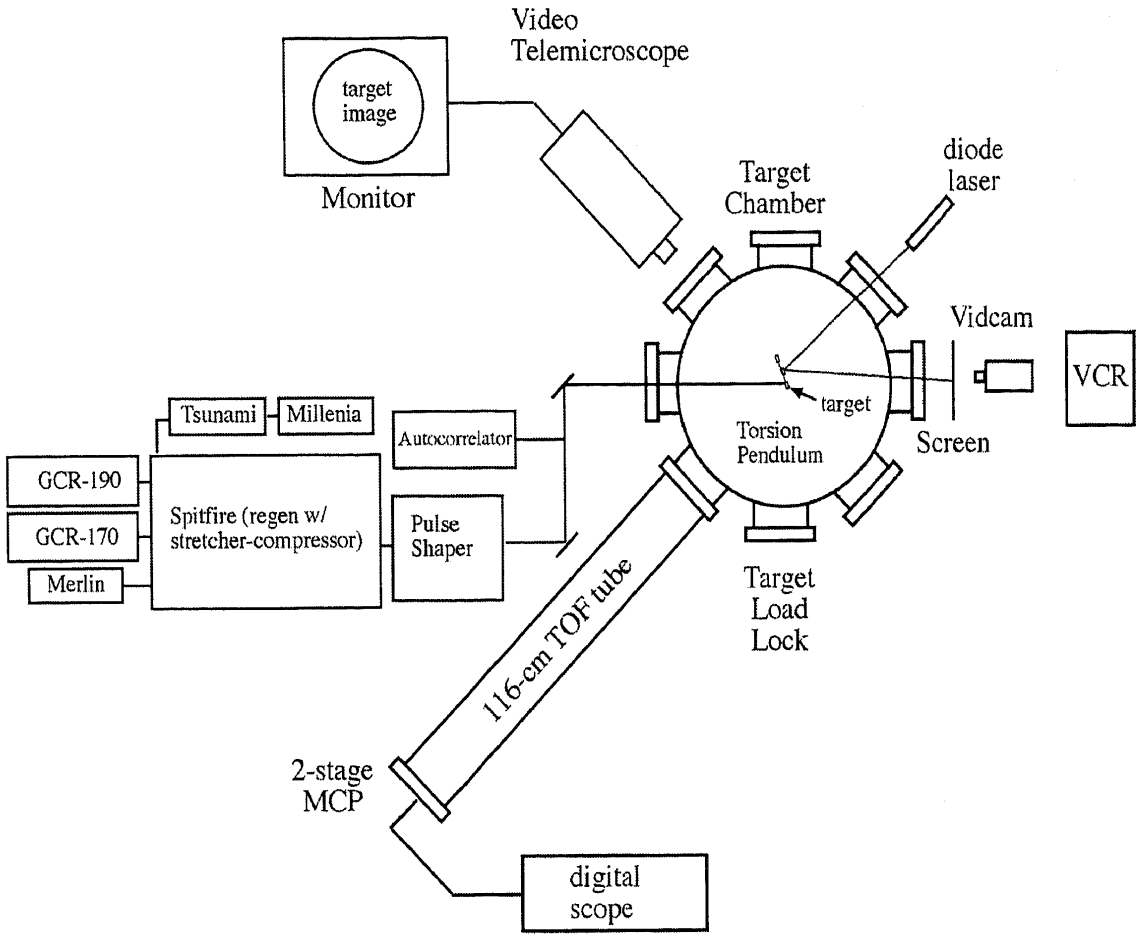

Figure 2. Setup for these experiments. Laser pulse duration was 130 fs.

target over a factor of 20. The design of our torsion pendulum has been reported elsewhere[8]. Its response was 0.681 dyn-s/rad. The nature of the impulse sensor limited us to single shot measurements. Target chamber pressure during measurements was 100μtorr. Angle of incidence on the target was 22°.

A total of 204 impulse data shots were taken on 10 materials. These were Li, Al, Mo, Fe, Zr, Au, W, and three energetic polymers which are of interest for the microthruster work, and which are described in detail in a companion paper[17]. Two of the polymers were doped with a tuned IR absorber centered at 915 and 935 nm, respectively, wavelengths appropriate for the microthruster application. The third used nanodisperse carbon as the laser absorber.

Ion time-of-flight (TOF) data was taken for each shot, using a Burle Instruments TOF detector with a two-stage microchannel plate (MCP). MCP voltage varied from 1250 to 1900V depending on the ion flux. The ablation laser

was incident at 22° on plane, circular targets. Polarization was s-plane, but the near-normal angle of incidence makes the polarization state of mainly academic interest. The axis of the TOF tube was inclined at 22° to the target surface normal.

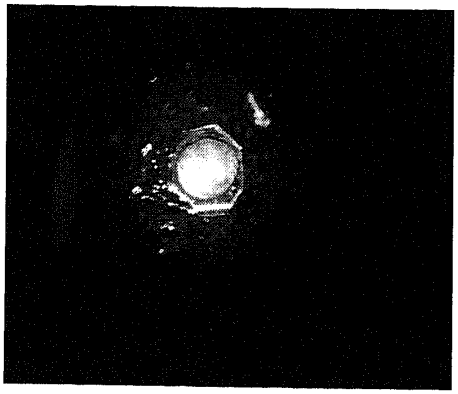

Figure 3. Illustrating successful target alignment with a 1-mm target. The bright area in the center of the target is the result of about 20 shots.

To generate useful physics data, we were careful to make target size closely match ablation beam size on the target. Targets which are larger than the beam spacially integrate the expanding blast wave, adding momentum which is geometry-dependent rather than a basic property of the interaction. Targets were 5.0 and 1.0 mm in diameter; matching beam diameters at $1/e^2$ intensity were 4.44 and 1.07 mm, respectively. Beam distributions were measured using the varying intensity fixed threshold method[18].

Targets were attached to the torsion pendulum with vacuum grease and manually aligned to within ±100μm transverse accuracy to the ablation beam [Figure 3]. Nevertheless, alignment errors were responsible for some scatter in the results obtained.

Axial displacement could be controlled to within 10μm by via the sharp depth of field of the video telemicroscope and a stepper-driven gearmotor which rotated the fiber supporting the target arm.

As many as 20 shots were taken on each target before replacement, since single shot etch depth was less than 3nm per pulse.

Several surface cleaning shots were taken prior to the data to remove grease and debris from the target surface.

Metallic targets were all certified equal to or better than 99.95% purity by their supplier, Alfa-Aesar. The organic targets were prepared as indicated in the companion paper[17], and used polyimide substrates.

Targets were mounted on both arms of the torsion pendulum to maximize data throughput per vacuum-to-air cycle.

4. RESULTS

Momentum Coupling Data

Figures 4-5 show typical impulse coupling results we obtained for two metals and one organic target. To counteract scatter, the impulse from as many as five single shots were numerically averaged to obtain one data point in the plot. The error bars show the range of the original data.

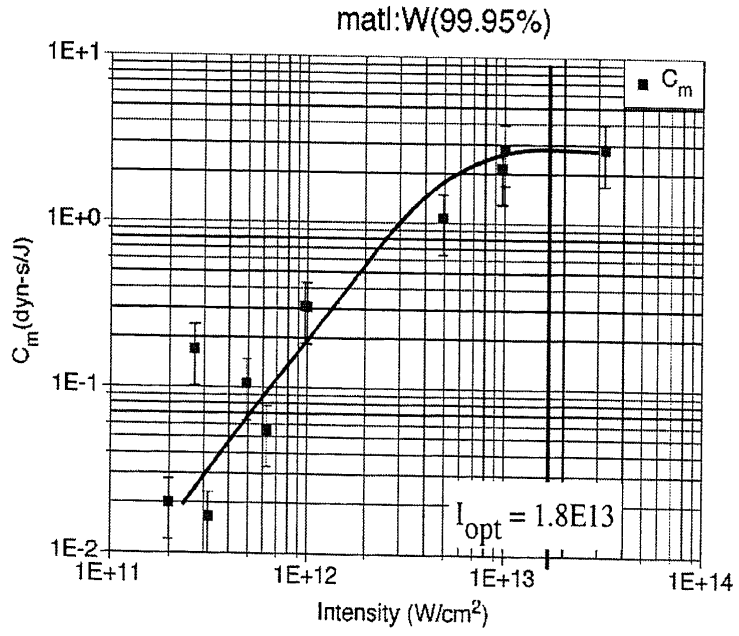

Figure 4. Impulse coupling data for tungsten.

A curve is drawn through the data to guide the eye, and the corresponding intensity for maximum impulse coupling efficiency, I_{opt}, is indicated on each plot. These new data points are then presented on the revised optimum fluence plot, Figure 6.

All results are summarized in Table 1. More detailed results will be presented in a later publication. In the Table, maximum exhaust velocity is drawn from the MCP TOF data which will be discussed in the next section.

Time of Flight Data

Although originally planned as a secondary measurement, the TOF data turned out to be at least as interesting as the primary momentum transfer data. Sometimes, the data demonstrated a single, high velocity peak.

Table 1. Results for impulse coupling and ion velocity at 130fs						
Material	Φ_{opt} (J/cm^2)	Expt'l C_{mopt} (dyn-s/J)	C_m predicted by Eq. (6)	Ion velocity predicted by Eq. (9)	Fast ion drift velocity (cm/s)	Slow ion drift velocity (cm/s)
Li	1.04	2.5	2.0	4.07 E6	1.80 E7	2.30 E6
Al	1.17	1.8	3.6	2.25 E6	1.50 E7	2.20 E6
Mo	0.78	4.2	6.2	1.29 E6	1.30 E7	2.40 E6
Au	1.37	1.8	8.5	9.43 E5	1.62 E7	2.35 E6
Fe	1.30	3.5	4.9	1.64 E6	1.40 E7	2.20 E6
W	2.34	2.5	8.2	9.71 E5	1.10 E7	3.05 E6
Lippert 915nm IR absorber:GAP	0.975	8.0	2.5	3.21 E6	6.80 E6	2.00 E6
Lippert 935nm IR absorber: GAP	1.30	3.2	2.5	3.21 E6	1.00 E7	3.23 E6
Lippert C:GAP	1.30	4.0	2.5	3.21 E6	5.70 E6	3.70 E6

More often, there were two or even three peaks [Figure 7]. In general, all the ion peaks could be fit reasonably well by a drifting thermal maxwellian.

In Figure 8, we have plotted the most probable thermal velocity

$$v_{th(p)} = 1.385E6\ (T_{eV}/A)^{1/2}\ cm/s \qquad (12)$$

where A is atomic mass, rather than the temperatures of the ions in the fast, medium and slow peaks in order to highlight the fact that this quantity is nearly constant across the large range of atomic mass studied. The parameter $v_{th(p)slow}$ decreases by a factor of 2 and v_{Dslow} is nearly constant as we go from Li to W targets. Figure 9 shows the variation of TOF parameters vs. intensity, for gold.

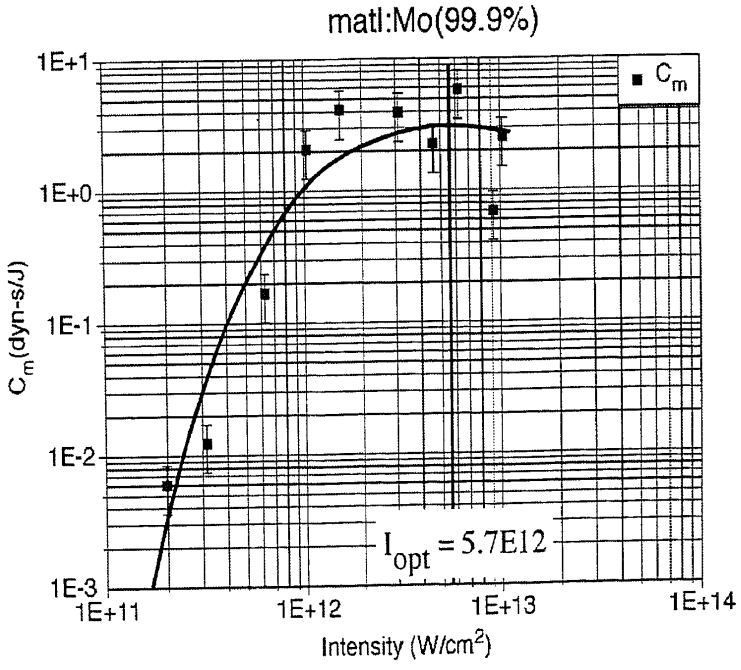

Figure 5. Impulse coupling data for molybdenum. A trendline is added to emphasize the meaning of the optimum coupling intensity concept.

Figure 10 shows that the impulse we measure scales proportionally to the total fast and slow ion flux.

5.0 DISCUSSION

Measured impulse coupling coefficients differ by as much as a factor of 5 from the prediction of Eq. (6) using Z=1 at 130fs. This is not surprising, since Ihlemann[16] has shown that Eq. (6) begins to fail for pulses shorter than about 10 ps.

Since mass analysis was not available for these measurements, there is some uncertainty in assigning identity to the ion peaks. The slow ion peak velocity is about 50% larger than that predicted by Eq. (9). The fast ion temperature we derive from the data fit in Fig. 7 is 10.4 keV if we assume the "fast" peak is due to Au, but only 53 eV if we assume it is due to H. This value is consistent with the temperatures derived for the "medium" and "slow" peaks, assuming the "medium" peak is due to oxygen. Similar results to those shown in Fig. 7

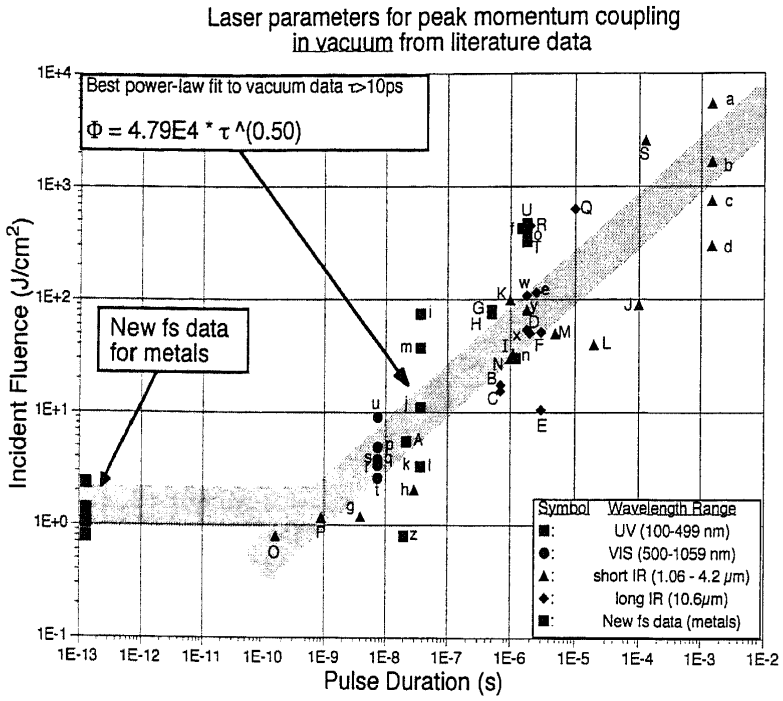

Figure 6. Revised optimum coupling fluence plot shows purely thermal behavior down to 100ps, and a flat behavior for shorter pulses.

were obtained for the other target materials [Table 1]. We found that the second peak became more dominant as intensity increased

We therefore take the fast ion peak to be due to hydrogen ions, and the medium velocity ("med") peak which is sometimes seen, as due to oxygen, arising from water vapor. The specific impulse values are not dramatically different from what one sees in ns-pulse work, or even[4] at 20ns.

Others have seen similar multiple peaks in TOF measurements. Ye, *et al.* from the Russo group at Lawrence Berkeley Laboratory studied laser ablation of Ti at 80fs and intensities similar to ours, and found 2-3 ion peaks with a fast ion drift velocity v_{Dfast} ~ 2E7 cm/s. Over a decade of incident intensity, v_{Dfast} varied less than a factor of two. They appeal to Coulomb explosion as the source of the first peak, which they assign to the target material ions. Features very similar to those we report were observed on Ti using a much lower base pressure (0.1μtorr) and a 3Hz shot rate.

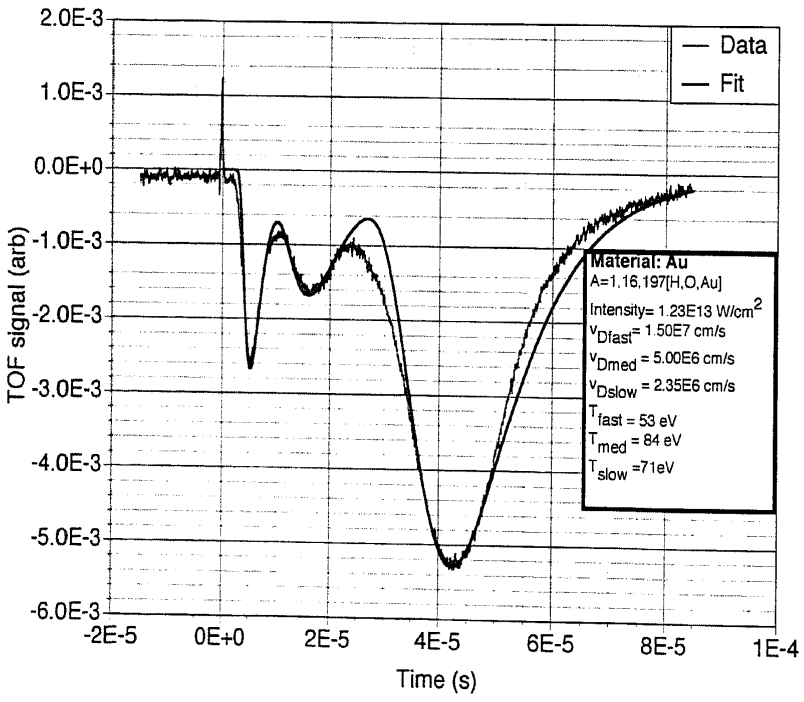

Figure 7. TOF data for gold, fit by individual drifting maxwellians. Drift velocities are 155, 0.55 and 0.26 km/s respectively for what we assume to be hydrogen, oxygen and gold ions. Temperatures for the three groups are 53, 84 and 71 eV, respectively.

Amoruso, *et al.*[20] reported double peaks from Au, Cu and Al illuminated by 120fs pulses, also around 10TW/cm². They noted the presence of H ions, and did do mass analysis, which showed that the hydrogen content never exceeded a few percent of the collected ion yield. They therefore conclude that the fast peaks are due to high energy target material ions rather than hydrogen. They found p-polarized light to be about 10 times more effective than s-polarized light in generating ions. However, with their 50° incidence angle, the distinction between polarization states is expected to be much more significant than in our case. They suggest that the second peak is due to a thermal process subsequent to energy relaxation over a few ps in the target surface. They call the first peak "nonthermal," referring to the process producing the peak. This is an unfortunate terminology, since we have shown in dozens of TOF data that each of

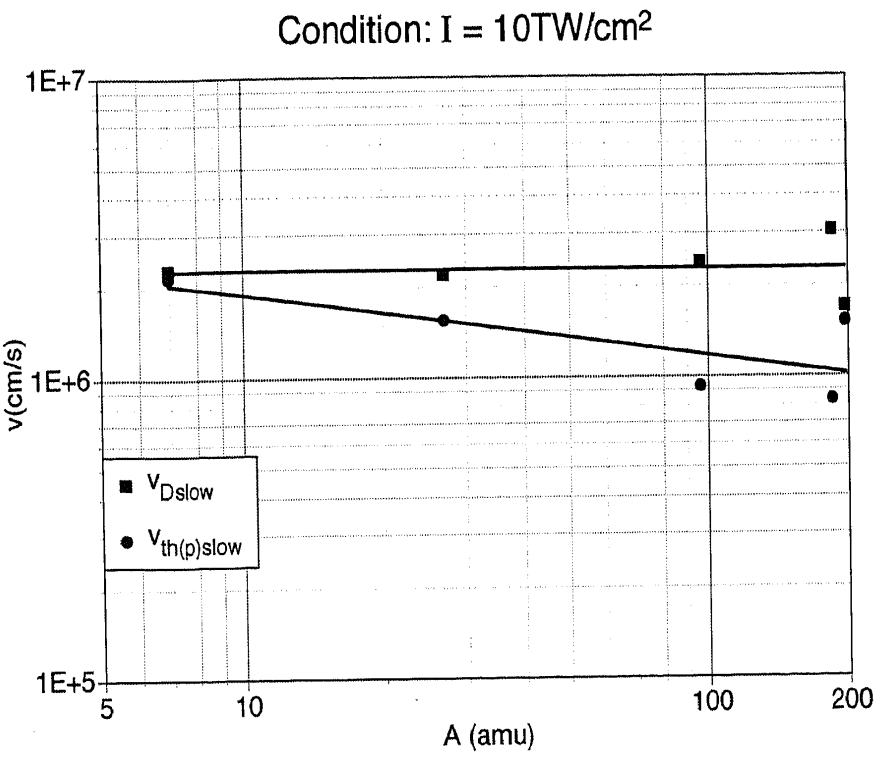

Figure 8. Variation of TOF ion parameters with atomic mass A, at 10TW/cm^2. Targets were Li, Al, Mo, Fe, Zr, Au and W. Here, we plot $v_{th(p)slow}$ (the most probable thermal velocities) rather than T_{slow} to eliminate the atomic mass dependence of the temperatures, which distracts from the point we wish to make. Only a slight variation of the ion velocities is seen. As atomic mass increases by a factor of 29, $v_{th(p)slow}$ decreases according to $A^{-0.21}$, and v_{Dslow} is nearly constant.

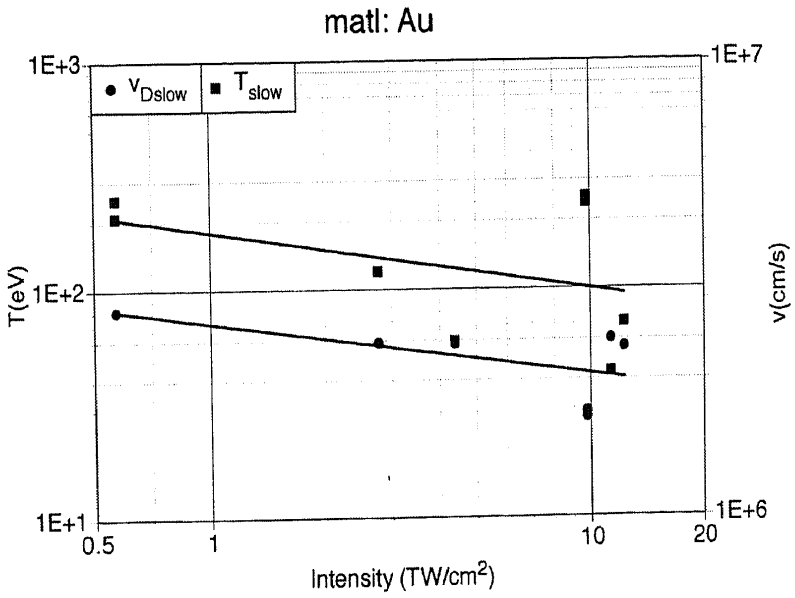

Figure 9. Variation of TOF ion parameters with intensity for gold. Only a slight variation is seen. Over a factor of 20 in incident intensity, T_{slow} decreases by a factor of 2 according to $I^{-0.25}$ and v_{Dslow} by a factor of 1.4, as $I^{-0.11}$.

the peaks observed can be fit with a drifting maxwellian with only slight error in all but a few instances.

Varel, *et al.*[21] made measurements on sapphire with 200fs pulses at up to 2TW/cm^2. Using a time-of-flight mass spectrometer, Al^+, O^+ and O^{2+} ions were observed. They consider a two-step process in which Coulomb explosion from ionized defect centers drives the first peak, followed by a thermal ion pulse which transports the bulk of neutral ablated material.

Pakhomov, *et al.*[22] made measurements of ion velocities generated by a number of materials at 100fs. They saw ion drift velocities decrease approximately according to $A^{-0.5}$, whereas our measurements showed $v_{th(p)slow}$ and v_{Dslow} nearly independent of A. The difference may be due to their high operating pressure of 3 millitorr, a condition for which the mean free path for ion collision with neutrals is on the order of 5cm.

We can say that the drift and thermal velocities we observed are nearly constant vs. atomic mass for all materials at 10TW/cm^2, and do not depend much on intensity either, for a single material.

This rather unexpected result indicates an ion acceleration process which emphasizes momentum conservation rather than energy conservation in the mechanism connecting the incident photons with accelerated charged particles leaving the target. This is true independent of assumptions made about the ion identities.

Examples of momentum-conserving processes are Coulomb explosion, as well as wave-wave interactions in a plasma, such as stimulated Raman scattering (SRS)[23].

Bulgakova, *et al.* have stated that theory predicts Coulomb explosion to be impossible for metals[24] because their higher electron mobility inhibits buildup of the required accelerating field.

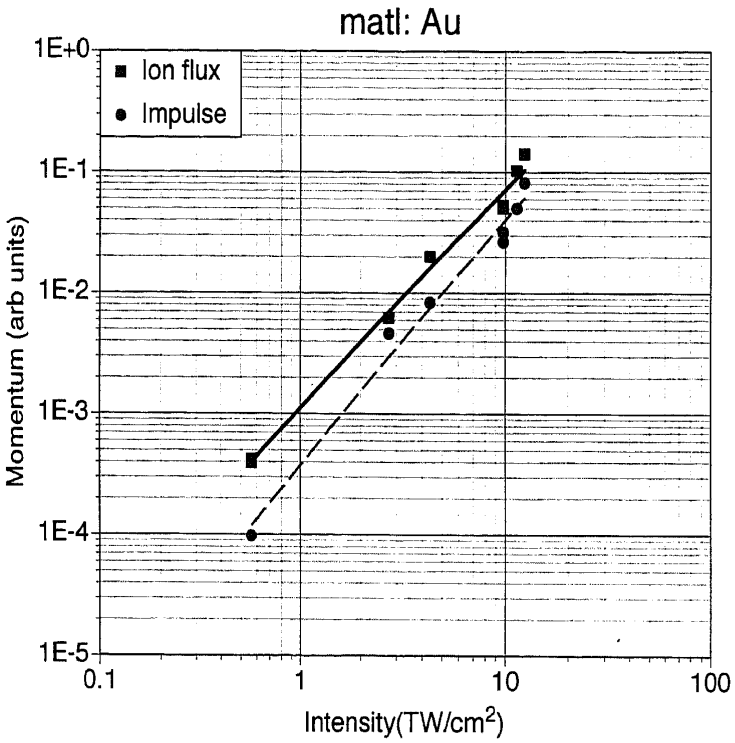

Figure 10. Impulse measured with the torsion pendulum correlates well with total ion flux over the intenstiy range studied.

We believe that more attention needs to be paid to plasma wave mechanisms in the ion acceleration process. We intend to resolve the mechanism for ion acceleration, and their identities, in a forthcoming paper.

6. SUMMARY

For the first time, we measured impulse generation at 130fs on several metals and three organic materials. To our knowledge, this is the first such measurement for pulses shorter than 100ps. We found the 130fs optimum coupling fluence to be essentially the same as that for 100ps. We also measured TOF signals for ions generated in the ablation experiments and found that drift velocities and temperatures changed very little over more than an order of magnitude intensity variation on a particular target material, or over the range from 7 to 200 amu at 10TW/cm^2. Generally, we found two to three peaks in the TOF signal, and that the second peak became more dominant as intensity increased.

We found that the measured impulse correlated well with the ion flux, determined by adding contributions from all the peaks.

ACKNOWLEDGMENTS

This work was supported by Photonic Associates' Internal Research and Development Fund. The thoughtful and effective assistance of the coauthors, their many helpful suggestions, and the use of the laboratory at Los Alamos is very gratefully acknowledged. We also acknowledge useful discussions with Dr. Razvan Stoian of the Max Born Institut.

REFERENCES

1. A. Kantrowitz, *Aeronaut. Astronaut.* **10**, 74 (1972)

2. C. Phipps and J. Luke, "Diode Laser-driven Microthrusters: A new departure for micropropulsion," *AIAA Journal* **40** (2) pp. 310-318 (2002)

3. L. Myrabo and Yu. Raizer, Paper 94-2451, AIAA Plasmadynamics and Lasers Conference, Colorado Springs, (1994)

4. C. Phipps and M. Michaelis, "Laser Impulse Space Propulsion", *Journal of. Laser and Particle Beams* vol.12 no. 1, pp. 23-54 (1994)

5. C. Phipps, J. Reilly and J. Campbell, "Optimum Parameters for Laser-launching Objects into Low Earth Orbit", J. *Laser and Particle Beams*, **18** no. 4 pp. 661-695 (2000)

6. C. Phipps and J. Luke, "Micro Laser Plasma Thrusters for Small Satellites", SPIE **4065**, pp 801-809 (2000)

7. D. Gonzales and R. Baker, "Microchip Laser Propulsion for Small Satellites", paper AIAA 2001-3789, *37th AIAA/ASME/SAE/ASEE Joint Propulsion Conference, Salt Lake City* (2001)

8. C. Phipps and J. Luke, "Diode Laser-driven Microthrusters: A new departure for micropropulsion," *AIAA Journal* **40** (2) pp. 310-318 (2002)

9. A. Pakhomov, D. Gregory and M. Thompson, "Specific impulse and other characteristics of elementary propellants for ablative laser propulsion," *AIAA Journal* **40** (5), 947-952 (2002)

10. T.Yabe, C.Phipps, K.Aoki, M.Yamaguchi, R.Nakagawa , H.Mine , Y.Ogata , C.Baasandash , M.Nakagawa, E.Fujiwara, K.Yoshida , A.Nishiguchi and I.Kajiwara, "Micro-airplane Propelled by Laser-Driven Exotic Target", *App. Phys. Lett.*, **80**, 4318-20 (2002)

11. C. R. Phipps, J. Luke and T. Lippert, "Laser ablation of organic coatings as a basis for micropropulsion", *Thin Solid Films,* **453-4**, 573-83 (2004)

12. C. Phipps, T. Turner, R. Harrison, G. York, W. Osborne, G. Anderson, X. Corlis, L. Haynes, H. Steele, K. Spicochi, and T. King, "Impulse Coupling to Targets in Vacuum by KrF, HF and CO_2 Lasers" , *Journal of. Applied. Physics.*, vol. 64, no. 3 pp. 1083-96 (1988)

13. C. Phipps and R. Dreyfus, "Laser ablation and plasma formation" in *Laser Ionization Mass Analysis,* Akos Vertes, Renaat Gijbels and Fred Adams, eds., Wiley, New York, May, (1993)

14. H.S. Carslaw and J.C. Jaeger, *Conduction of Heat in Solids*, 2nd ed. Clarendon Press, Oxford (1959) p. 75

15. C. R. Phipps, "Ultrashort Pulses for Impulse Generation in Laser Propulsion Applications", Thirteenth International Conference on Laser Interactions and Related Plasma Phenomena, *AIP Conference Proceedings* **406** pp. 477-484 (1997)

16. F. Beinhorn, J. Ihlemann, K. Luther and J. Troe, "Plasma effects in picosecond-femtosecond UV laser ablation of polymers," *Appl. Phys. A* to appear (2004)

17. T. Lippert, M. Hauer, L. Urech, A. Wokaun and E. Schmid, "Designed polymers for laser-based microthrusters-correlation of thrust with material, plasma and shockwave properties," SPIE **5448** to appear (2004)

18. I. M. Winer, "A Self-Calibrating Technique Measuring Laser Beam Intensity Distributions," *Appl. Opt.* **5**, 1437-1439 (1966)

19. M. Ye and C. Grigoropoulous, "Time-of-flight and emission spectroscopy study of femtosecond laser ablation of titanium," *J. Appl. Phys.* **89**, 5183-5190 (2001)

20. S. Amoruso, X. Wang, C. Altucci, C. de Lisio, M. Armenante, R. Bruzzese and R. Velotta, "Thermal and nonthermal ion emission during high-fluence femtosecond laser ablation of metallic targets," *Appl. Phys. Lett.* **77**, 3728-30 (2000)

21. H. Varel, M. Wähmer, A. Rosenfeld, D. Ashkenasi and E Campbell, "Femtosecond laser ablation of sapphire: time-of-flight analysis of ablation plume," *Appl. Surf. Sci.* **127**, 128-133 (1998)

22. A. Pakhomov, A. Roybal and M. Duran, "Ion dynamics of plasmas induced in elemental targets by femtosecond laser radiation," *Applied Spectroscopy* **53**, 979-986 (1999).

23. K. Estabrook, W. Kruer and B. Lasinski, "Heating by Raman Backscatter and Forward Scatter," *Phys. Rev. Lett.* **45** 1399-1403 (1980)

24. N. Bulgakova, R. Stoian, A. Rosenfeld, W. Marine and E. Campbell, "A general continuum approach to describe fast electronic transport in pulsed laser irradiated materials: the problem of Coulomb explosion," SPIE **5448**, to appear (2004)